Supplementary Information

Polarized Raman spectroscopy study of CVD-grown Cr_2S_3 flakes: Unambiguous identification of phonon modes

Anabil Gayen[1,2], Gwang Hwi An[1], Ikhwan Nur Rahman[1], Min Choi[1], Qoimatul Mustaghfiroh[1], Prashant Vijay Gaikwad[1,2], Evan S. H. Kang[1], Kyoung-Ho Kim[1,2], Chuyang Liu[3], Kyung Wan Kim[1,2*], Junhyeok Bang[1,2**], Hyun Seok Lee[1,2***] and Dong-Hyun Kim[1,2****]

[1]*Department of Physics, Chungbuk National University, Cheongju 28644, Korea*

[2]*Research Institute for Nanoscale Science and Technology, Chungbuk National University, Cheongju 28644, Korea*

[3]*School of Materials Science and Technology, Nanjing University of Aeronautics and Astronautics, Nanjing, 211106, China*

*Corresponding authors' emails: * kyungwan@chungbuk.ac.kr, **jbang@cbnu.ac.kr, ***hsl@chungbuk.ac.kr, ****donghyun@cbnu.ac.kr*

Section 1: Schematic Diagram of CVD process:

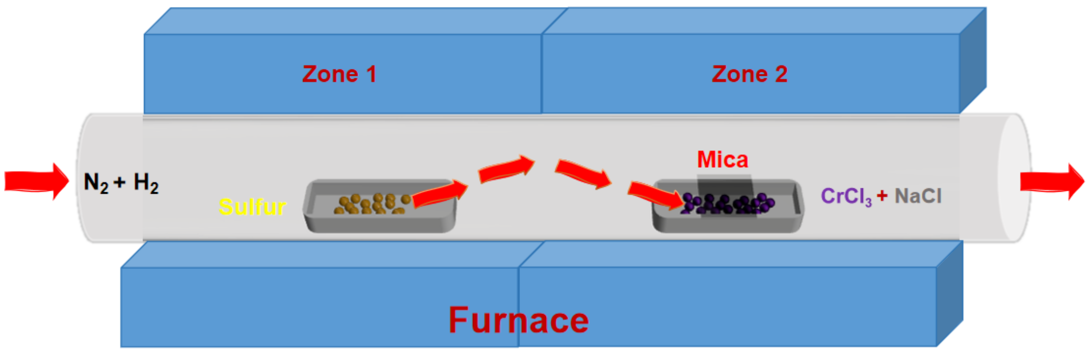

Figure S1. Schematic diagram of the set-up used for CVD growth of 2D Cr_2S_3 nanoflakes.

Section 2: Examination of the quality and uniformity of the CVD-grown Cr_2S_3 nanoflakes:

(a)

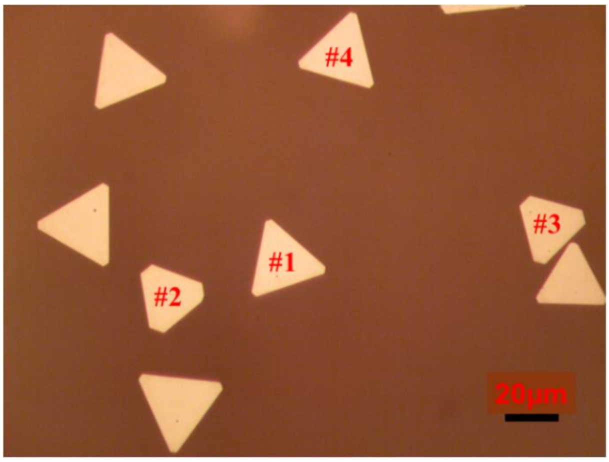

(b)

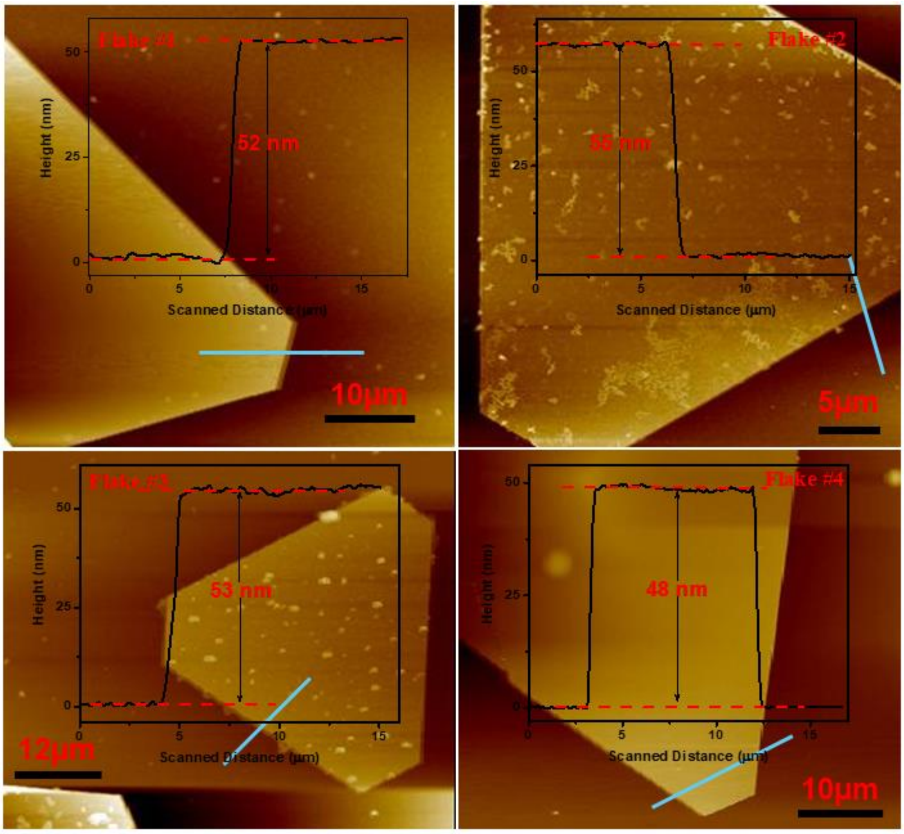

Figure S2. (a) Optical microscope image of CVD-grown 2D Cr_2S_3 on mica substrate, where four different flakes are numbered; **(b)** AFM images of those four numbered flakes together with their respective height profiles.

Section 3: AFM images and corresponding height profiles of CVD-grown 2D Cr_2S_3 nanoflakes having different thicknesses:

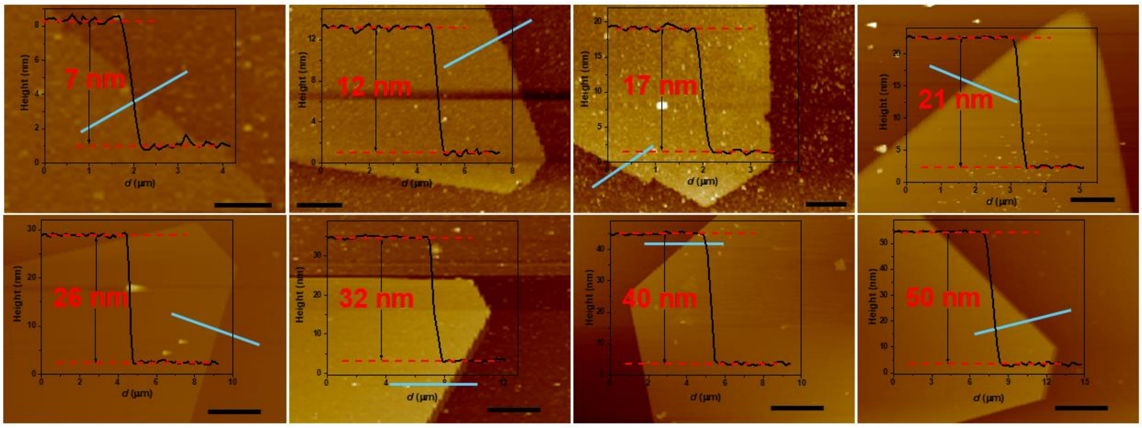

Figure S3. AFM images and corresponding height profiles of CVD-grown 2D Cr_2S_3 nanoflakes having different thicknesses used for thickness dependent Raman study in Fig. 2(b) of main text. The scale bar for the four images in the first row is 2 μm and that is for the second row is 8 μm.

Section 4: Deconvolution of closely placed Raman modes, P_1 and P_2, over the wide temperature regime:

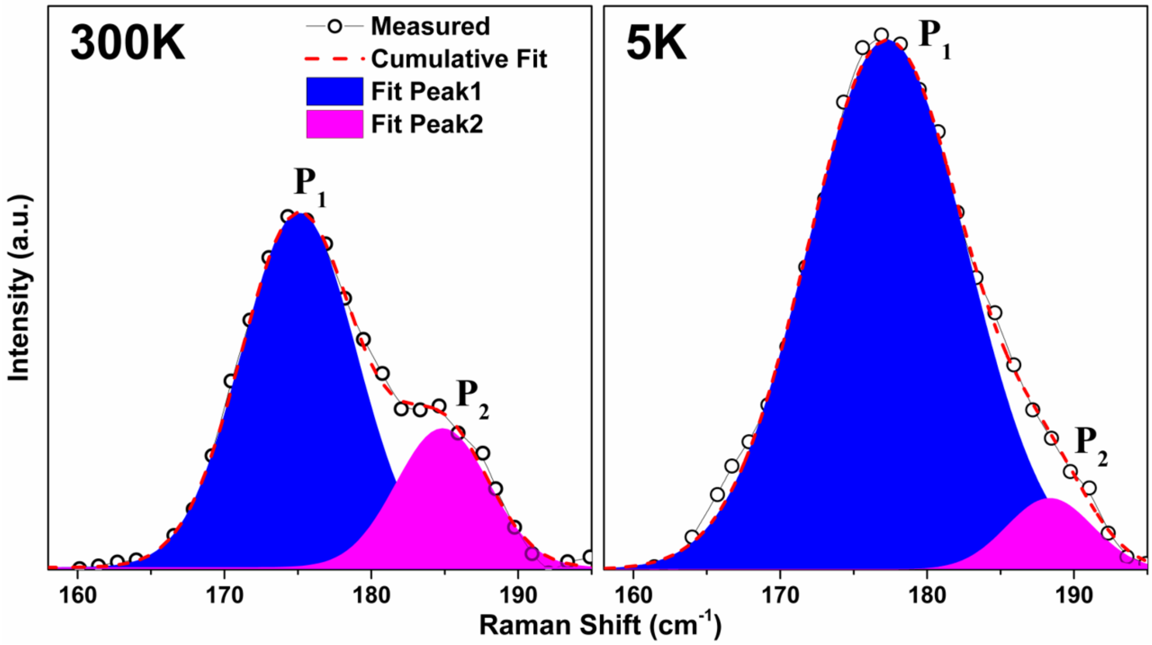

Figure S4. Deconvolution of two closely placed modes, P_1 and P_2, at temperatures 300K and 5K.

Section 5: Schematic diagrams of different polarized Raman spectroscopy setup:

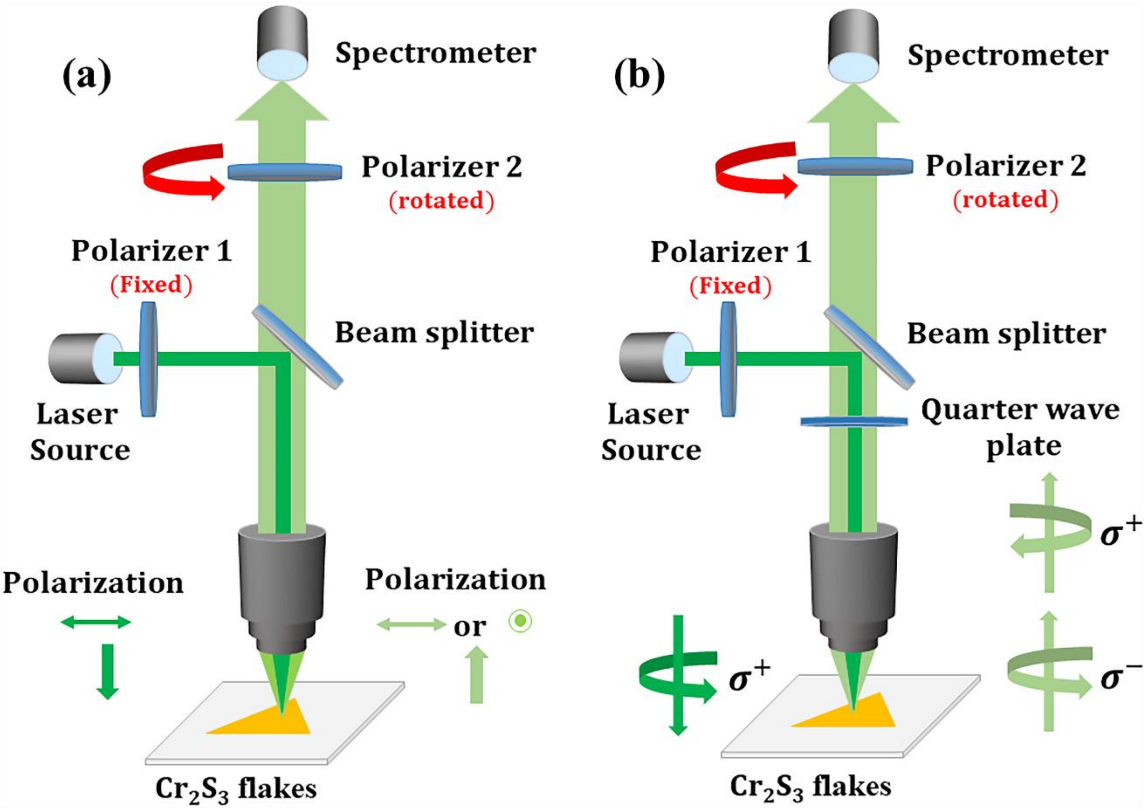

Figure S5. Schematic diagram of the experimental setup for, **(a)** linearly polarized Raman spectroscopy; **(b)** circularly polarized Raman spectroscopy.

Section 6: Raman spectroscopy results, for linearly polarized light, at different temperatures; Schematic of ARPRS setup:

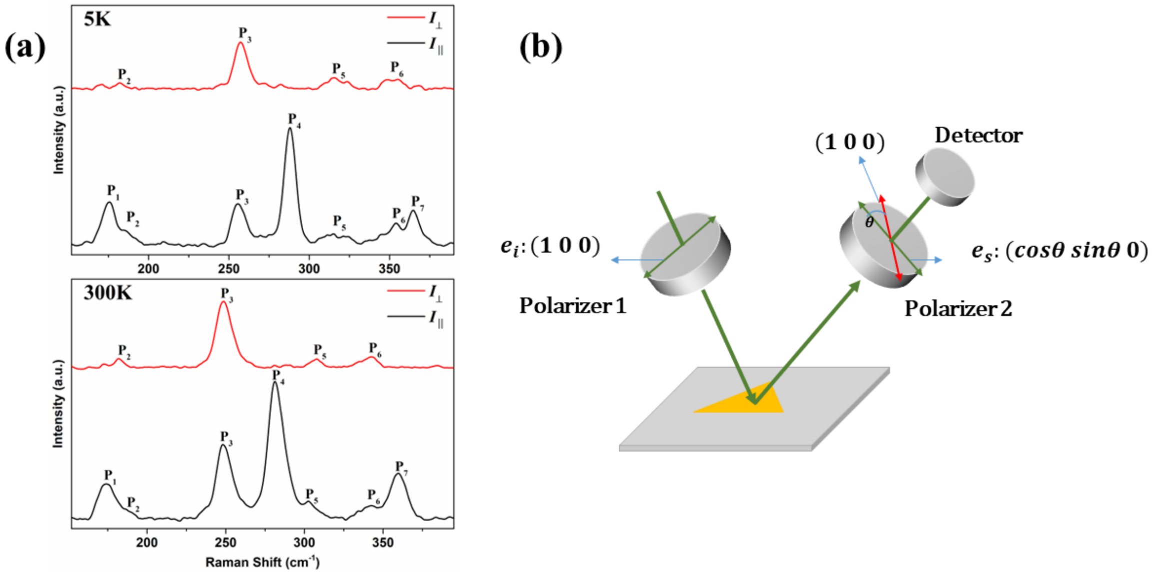

Figure S6. (a) Linearly polarized Raman spectroscopy for parallel (||) and perpendicular (⊥) configurations measured at 5K and 300K; **(b)** Schematic diagram of the experimental setup for Angle resolved polarized Raman spectroscopy.

Section 7: Table containing the first-order temperature coefficient (χ) values of various 2D materials:

Table S1: Comparison of the first-order temperature coefficient (χ) value for various 2D materials including this work:

Materials	Raman modes	χ ($cm^{-1}K^{-1}$)	References
Monolayer graphene	G	–0.0162	1
Bilayer graphene	G	–0.0154	
Monolayer MoS_2	A_{1g}	–0.013	2
	E_{2g}	–0.011	
Few-layer MoS_2	A_{1g}	–0.0123	3
	E_{2g}	–0.0132	
Few-layer black phosphorus	A_{1g}	−0.023	4
	A_{2g}	−0.018	
	B_{2g}	−0.023	
Few-layer WS_2	A_{1g}	−0.004	5
	E_{2g}	−0.008	
ZrSiS single crystals	E_g^1	−0.008	6
	E_g^2	−0.009	
	E_g^3	−0.015	
	A_{1g}^1	−0.012	
	A_{1g}^2	−0.012	
	B_{1g}	−0.014	
2D SnTe nanosheets	A_{1g}	−0.0183	7
	E_{2g}	−0.0141	
15 nm γ-Ga_2S_3 flakes	A_{1g}	−0.0073	8
CVD-grown Cr_2S_3	E_g (~247.4 cm^{-1})	-0.0103	9
	A_g (~281 cm^{-1})	-0.0066	
	A_g (~355.5 cm^{-1})	-0.0105	
50 nm thick Cr_2S_3	A_g (~175.1 cm^{-1})	-0.0093	This work
	E_g (~184.8 cm^{-1})	-0.0099	
	E_g (~250.1 cm^{-1})	-0.0235	
	A_g (~283.1 cm^{-1})	-0.0174	
	A_g (~360.2 cm^{-1})	-0.0210	

Section 8: Calculation details of Optical Selection Rule based on crystal symmetry dependent Raman Tensor:

Part 1:

The intensity of a Raman active mode with Raman tensor, Rj can be deduced by,

$$I \propto \sum_j \left| e_s^{\dagger} . R_j . e_i \right|^2$$

Where e_i and e_s are polarization vectors of the incident and scattered light.

The corresponding Raman tensors for Rhombohedral Cr_2S_3 belonging to R$\bar{3}$ space group (No. 148) are as follows:

$$\boldsymbol{A_g} = \begin{pmatrix} a & 0 & 0 \\ 0 & a & 0 \\ 0 & 0 & b \end{pmatrix};\ \boldsymbol{E_g} = \begin{pmatrix} c & d & e \\ d & -c & f \\ e & f & 0 \end{pmatrix}, \begin{pmatrix} d & -c & -f \\ -c & -d & e \\ -f & e & 0 \end{pmatrix}$$

For linearly parallel polarization configuration (||), the incident and scattered polarization vectors are:

$$e_i = \begin{pmatrix} 1 \\ 0 \\ 0 \end{pmatrix};\quad e_s = \begin{pmatrix} 1 \\ 0 \\ 0 \end{pmatrix}$$

The corresponding Raman intensities of Raman active modes are:

$$\boldsymbol{I}_{\parallel}\left(\boldsymbol{A}_{\boldsymbol{g}}\right) \propto \left|\begin{pmatrix}1 & 0 & 0\end{pmatrix}\begin{pmatrix}a & 0 & 0\\0 & a & 0\\0 & 0 & b\end{pmatrix}\begin{pmatrix}1\\0\\0\end{pmatrix}\right|^2 = \left|\begin{pmatrix}1 & 0 & 0\end{pmatrix}\begin{pmatrix}a\\0\\0\end{pmatrix}\right|^2$$

$$= |\boldsymbol{a}|^{2}$$

$$\boldsymbol{I}_{\parallel}\left(\boldsymbol{E}_{\boldsymbol{g}}\right) \propto \left|\begin{pmatrix}1 & 0 & 0\end{pmatrix}\begin{pmatrix}c & d & e\\d & -c & f\\e & f & 0\end{pmatrix}\begin{pmatrix}1\\0\\0\end{pmatrix}\right|^2 +$$

$$\left|\begin{pmatrix}1 & 0 & 0\end{pmatrix}\begin{pmatrix}d & -c & -f\\-c & -d & e\\-f & e & 0\end{pmatrix}\begin{pmatrix}1\\0\\0\end{pmatrix}\right|^2$$

$$= \left|\begin{pmatrix}1 & 0 & 0\end{pmatrix}\begin{pmatrix}c\\d\\e\end{pmatrix}\right|^2 + \left|\begin{pmatrix}1 & 0 & 0\end{pmatrix}\begin{pmatrix}d\\-c\\-f\end{pmatrix}\right|^2 = |\boldsymbol{c}|^{2} + |\boldsymbol{d}|^{2}$$

For linearly perpendicular polarization configuration ($\perp$), the polarization vectors for the incident and scattered light vectors are:

$$e_i = \begin{pmatrix}1\\0\\0\end{pmatrix}; \quad e_s = \begin{pmatrix}0\\1\\0\end{pmatrix}$$

The corresponding Raman intensities of Raman active modes for linearly perpendicular polarization configuration are:

$$\boldsymbol{I}_{\perp}\left(\boldsymbol{A}_{\boldsymbol{g}}\right) \propto$$

$$\left|\begin{pmatrix}0 & 1 & 0\end{pmatrix}\begin{pmatrix}a & 0 & 0\\0 & a & 0\\0 & 0 & b\end{pmatrix}\begin{pmatrix}1\\0\\0\end{pmatrix}\right|^2 = \left|\begin{pmatrix}0 & 1 & 0\end{pmatrix}\begin{pmatrix}a\\0\\0\end{pmatrix}\right|^2 = \mathbf{0}$$

$$\boldsymbol{I}_{\perp}(\boldsymbol{E_g}) \propto \left|\begin{pmatrix} 0 & 1 & 0 \end{pmatrix}\begin{pmatrix} c & d & e \\ d & -c & f \\ e & f & 0 \end{pmatrix}\begin{pmatrix} 1 \\ 0 \\ 0 \end{pmatrix}\right|^2 + \left|\begin{pmatrix} 0 & 1 & 0 \end{pmatrix}\begin{pmatrix} d & -c & -f \\ -c & -d & e \\ -f & e & 0 \end{pmatrix}\begin{pmatrix} 1 \\ 0 \\ 0 \end{pmatrix}\right|^2$$

$$= \left|\begin{pmatrix} 0 & 1 & 0 \end{pmatrix}\begin{pmatrix} c \\ d \\ e \end{pmatrix}\right|^2 + \left|\begin{pmatrix} 0 & 1 & 0 \end{pmatrix}\begin{pmatrix} d \\ -c \\ -f \end{pmatrix}\right|^2 = |\boldsymbol{c}|^2 + |\boldsymbol{d}|^2$$

<u>Part 2:</u>

Calculations for Angle Resolved Polarized Raman spectra (ARPRS):

For Angle Resolved Polarized Raman spectra, the intensities for both $\boldsymbol{A_g}$ and $\boldsymbol{E_g}$ modes can be calculated using the same formula:

$$I \propto \sum_j \left| e_s^{\dagger} . R_j . e_i \right|^2$$

In this configuration the incident and scattered polarization vectors are:

$$e_i = \begin{pmatrix} 1 \\ 0 \\ 0 \end{pmatrix} ; e_s = \begin{pmatrix} \cos\theta \\ \sin\theta \\ 0 \end{pmatrix} \qquad \boldsymbol{;\ \theta : 0^\circ \quad 90^\circ}$$

$$\qquad \qquad \parallel \quad \perp$$

$$\boldsymbol{I(A_g)} \propto \left|\begin{pmatrix}\cos\theta & \sin\theta & 0\end{pmatrix}\begin{pmatrix}a & 0 & 0\\ 0 & a & 0\\ 0 & 0 & b\end{pmatrix}\begin{pmatrix}1\\0\\0\end{pmatrix}\right|^2 =$$

$$\left|\begin{pmatrix}\cos\theta & \sin\theta & 0\end{pmatrix}\begin{pmatrix}a\\0\\0\end{pmatrix}\right|^2 = \boldsymbol{a^2\cos^2\theta}$$

$$\boldsymbol{I(E_g)} \propto \left|\begin{pmatrix}\cos\theta & \sin\theta & 0\end{pmatrix}\begin{pmatrix}c & d & e\\ d & -c & f\\ e & f & 0\end{pmatrix}\begin{pmatrix}1\\0\\0\end{pmatrix}\right|^2 +$$

$$\left|\begin{pmatrix}\cos\theta & \sin\theta & 0\end{pmatrix}\begin{pmatrix}d & -c & -f\\ -c & -d & e\\ -f & e & 0\end{pmatrix}\begin{pmatrix}1\\0\\0\end{pmatrix}\right|^2$$

$$= \left|\begin{pmatrix}\cos\theta & \sin\theta & 0\end{pmatrix}\begin{pmatrix}c\\d\\e\end{pmatrix}\right|^2 + \left|\begin{pmatrix}\cos\theta & \sin\theta & 0\end{pmatrix}\begin{pmatrix}d\\-c\\-f\end{pmatrix}\right|^2 =$$

$$|c\cos\theta + d\sin\theta|^2 + |d\cos\theta - c\sin\theta|^2$$

$$= \boldsymbol{c^2 + d^2}$$

Part 3:

Calculations for Polarized Raman spectra with circularly polarized light:

The helicity selection rule can be determined by the Raman tensor (**R_j**), The calculated Raman intensity is determined by:

$$I \propto \sum_j \left|\sigma_s^{\dagger}.R_j.\sigma_i\right|^2$$

Where $\boldsymbol{\sigma_s}$ and $\boldsymbol{\sigma_i}$ are the incident and scattered circularly polarized vectors.

Polarization vectors for left (σ+) and right (σ−) circularly polarized light are:

$$\sigma^+ = \frac{1}{\sqrt{2}}\begin{pmatrix}1\\i\\0\end{pmatrix};\sigma^- = \frac{1}{\sqrt{2}}\begin{pmatrix}1\\-i\\0\end{pmatrix}$$

Hence, the intensities for $\boldsymbol{A_g}$ and $\boldsymbol{E_g}$ modes for both helicity conserved (σ+σ+) and helicity changed (σ+σ−) cases can be calculated as:−

For helicity conserved case (σ+σ+):

$$\boldsymbol{I_{\sigma+\sigma+}}\left(\boldsymbol{A_g}\right) \propto$$

$$\left|\frac{1}{2}\begin{pmatrix}1 & -i & 0\end{pmatrix}\begin{pmatrix}a & 0 & 0\\0 & a & 0\\0 & 0 & b\end{pmatrix}\begin{pmatrix}1\\i\\0\end{pmatrix}\right|^2 = \left|\frac{1}{2}\begin{pmatrix}1 & -i & 0\end{pmatrix}\begin{pmatrix}a\\ai\\0\end{pmatrix}\right|^2$$

$$= \left|\frac{1}{2}(a + a + 0)\right|^2 = |a|^2$$

$$\boldsymbol{I}_{\boldsymbol{\sigma+\sigma+}}\left(\boldsymbol{E}_{\boldsymbol{g}}\right) \propto \left|\frac{1}{2}\begin{pmatrix}1 & -i & 0\end{pmatrix}\begin{pmatrix}c & d & e\\ d & -c & f\\ e & f & 0\end{pmatrix}\begin{pmatrix}1\\ i\\ 0\end{pmatrix}\right|^2 + \left|\frac{1}{2}\begin{pmatrix}1 & -i & 0\end{pmatrix}\begin{pmatrix}d & -c & -f\\ -c & -d & e\\ -f & e & 0\end{pmatrix}\begin{pmatrix}1\\ i\\ 0\end{pmatrix}\right|^2 =$$

$$\left|\frac{1}{2}\begin{pmatrix}1 & -i & 0\end{pmatrix}\begin{pmatrix}c+id\\ d-ic\\ e+if\end{pmatrix}\right|^2 + \left|\frac{1}{2}\begin{pmatrix}1 & -i & 0\end{pmatrix}\begin{pmatrix}d-ic\\ -c-id\\ -f+ie\end{pmatrix}\right|^2 =$$

$$\left|\frac{1}{2}(c+id-id-c)\right|^2 + \left|\frac{1}{2}(d-ic+ic-d)\right|^2 = 0$$

For helicity changed case (σ+σ−):

$$\boldsymbol{I}_{\boldsymbol{\sigma+\sigma-}}\left(\boldsymbol{A}_{\boldsymbol{g}}\right) \propto$$

$$\left|\frac{1}{2}\begin{pmatrix}1 & i & 0\end{pmatrix}\begin{pmatrix}a & 0 & 0\\ 0 & a & 0\\ 0 & 0 & b\end{pmatrix}\begin{pmatrix}1\\ i\\ 0\end{pmatrix}\right|^2 = \left|\frac{1}{2}\begin{pmatrix}1 & i & 0\end{pmatrix}\begin{pmatrix}a\\ ai\\ 0\end{pmatrix}\right|^2 =$$

$$\left|\frac{1}{2}(a-a+0)\right|^2 = 0$$

$$\boldsymbol{I}_{\boldsymbol{\sigma+\sigma-}}\left(\boldsymbol{E}_{\boldsymbol{g}}\right) \propto \left|\frac{1}{2}\begin{pmatrix}1 & i & 0\end{pmatrix}\begin{pmatrix}c & d & e\\ d & -c & f\\ e & f & 0\end{pmatrix}\begin{pmatrix}1\\ i\\ 0\end{pmatrix}\right|^2 + \left|\frac{1}{2}\begin{pmatrix}1 & i & 0\end{pmatrix}\begin{pmatrix}d & -c & -f\\ -c & -d & e\\ -f & e & 0\end{pmatrix}\begin{pmatrix}1\\ i\\ 0\end{pmatrix}\right|^2 =$$

$$\left|\frac{1}{2}\begin{pmatrix}1 & i & 0\end{pmatrix}\begin{pmatrix}c+id\\ d-ic\\ e+if\end{pmatrix}\right|^2 + \left|\frac{1}{2}\begin{pmatrix}1 & i & 0\end{pmatrix}\begin{pmatrix}d-ic\\ -c-id\\ -f+ie\end{pmatrix}\right|^2 =$$

$$\left|\frac{1}{2}(c+id+c+id)\right|^2 + \left|\frac{1}{2}(d-ic-ic+d)\right|^2 = \mathbf{2(c^2+d^2)}$$

References

[1] I. Calizo, A.A. Balandin, W. Bao, F. Miao, and C. N. Lau, *Temperature Dependence of the Raman Spectra of Graphene and Graphene Multilayers*, Nano Lett., 7, 2645 (2007).

[2] R. Yan, J.R. Simpson, S. Bertolazzi, J. Brivio, M. Watson, X. Wu, A. Kis, T. Luo, A.R. Hight Walker, and H.G. Xing, *Thermal Conductivity of Molybdenum Disulfide Obtained from Temperature-Dependent Raman Spectroscopy*, ACS Nano 8, 986 (2014).

[3] S. Sahoo, A.P.S. Gaur, M. Ahmadi, M.J.-F. Guinel, and R.S. Katiyar, *Temperature-Dependent Raman Studies and Thermal Conductivity of Few-Layer* MoS_2, J. Phys. Chem. C 117, 9042 (2013).

[4] S. Zhang, J. Yang, R. J. Xu, F. Wang, W. F. Li, M. Ghufran, Y. W. Zhang, Z. F. Yu, G. Zhang, Q. H. Qin and Y. R. Lu, *Extraordinary Photoluminescence and Strong Temperature/Angle-Dependent Raman Responses in Few-Layer Phosphorene*, ACS Nano, 8, 9590 (2014).

[5] M. Thripuranthaka, R.V. Kashid, C.S. Rout, D.J. Late, *Temperature dependent Raman spectroscopy of chemically derived few layer* MoS_2 *and* WS_2 *nanosheets*, Appl. Phys. Lett. 104, 081911 (2014).

[6] W. Zhou, H. Gao, J. Zhang, R. Fang, H. Song, T. Hu, A. Stroppa, L. Li, X. Wang, S. Ruan, and W. Ren, *Lattice dynamics of Dirac node-line semimetal ZrSiS*, Phys. Rev. B 96, 064103 (2017).

[7] Y. Su, C. Ding, Y. Yao, R. Fu, M. Xu, X. Liu, J. Lin, F. Wang, X. Zhan and Z. Wang, *Orietation-controlled synthesis and Raman study of 2D SnTe*, Nanotechnology 34, 505206 (2023).

[8] N. Zhou, L. Gan, R. Yang, F. Wang, L. Li, Y. Chen, D. Li, and T. Zhai, *Nonlayered Two-Dimensional Defective Semiconductor* γ-Ga_2S_3 *toward Broadband Photodetection*, ACS Nano 13, 6297 (2019).

[9] S. Zhou, R. Wang, J. Han, D. Wang, H. Li, L. Gan, and Tianyou Zhai, *Ultrathin Non-van der Waals Magnetic Rhombohedral* Cr_2S_3*: Space-Confined Chemical Vapor Deposition Synthesis and Raman Scattering Investigation*, Adv. Funct. Mater. 29, 1805880 (2019).

*****